A TRIDENT SCHOLAR PROJECT REPORT

NO. 492

Optimizing the Structural and Deflagration Properties of Aluminum-Rich Paraffin-Based Hybrid Rocket Motors

by

Midshipman 1/C Kaden C. Dohm, USN

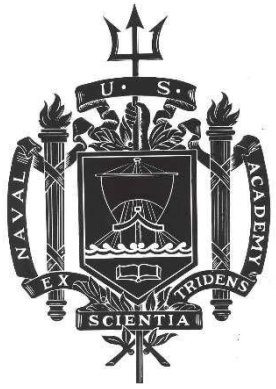

UNITED STATES NAVAL ACADEMY
ANNAPOLIS, MARYLAND

USNA-1531-2

REPORT DOCUMENTATION PAGE

Form Approved
OMB No. 0704-0188

1. REPORT DATE *(DD-MM-YYYY)*	**2. REPORT TYPE**	**3. DATES COVERED** *(From - To)*
7/6/20		

4. TITLE AND SUBTITLE
Optimizing the Structural and Deflagration Properties of Aluminum-Rich Paraffin-Based Hybrid Rocket Motors

5a. CONTRACT NUMBER

5b. GRANT NUMBER

5c. PROGRAM ELEMENT NUMBER

6. AUTHOR(S)
Dohm, Kaden C.

5d. PROJECT NUMBER

5e. TASK NUMBER

5f. WORK UNIT NUMBER

7. PERFORMING ORGANIZATION NAME(S) AND ADDRESS(ES)

8. PERFORMING ORGANIZATION REPORT NUMBER

9. SPONSORING / MONITORING AGENCY NAME(S) AND ADDRESS(ES)
U.S. Naval Academy
Annapolis, MD 21402

10. SPONSOR/MONITOR'S ACRONYM(S)

11. SPONSOR/MONITOR'S REPORT NUMBER(S)
Trident Scholar Report no. 492 (2020)

12. DISTRIBUTION / AVAILABILITY STATEMENT

This document has been approved for public release; its distribution is UNLIMITED.

13. SUPPLEMENTARY NOTES

14. ABSTRACT

Hybrid rocket motors offer an alternative to conventional solid motors and liquid engines. One of the most severe limiting factors of hybrid rocketry is the low regression rate as the fuel does not burn nearly as quickly as in a solid rocket. However, the discovery of liquefying fuels such as paraffin has greatly improved the regression rate of hybrid rocket fuels. Such fuels operate by liquefying to a greater extent than conventional fuels, whereby the low viscosity allows droplets of the fuel to become entrained in the oxidizer flow which increases the speed of the combustion process. Paraffin has a low compression strength and fractures easily. Recent studies show that the incorporation of polyethylene and aluminum powder can maintain and even increase the high regression rate of paraffin rocket motors, and increase the structural strength to allow these motors to survive the flight loads they experience during launch. This project seeks to further advance the benefits of the addition of aluminum powder as previous research suggests that the addition of aluminum powder at a concentration greater than 25% by mass could greatly increase the regression rate. As the concentration of aluminum powder increases more energy is released from the combustion of the fuel which increases the temperature of the combustion resulting in a faster regression rate, but the fuel also becomes more viscous which prevents the entrainment of fuel droplets which serves to limit the regression rate. Due to the COVID-19 pandemic, test fires were unable to be completed to measure the regression rate of the fuel samples with a higher concentration of aluminum powder. However, data from compressive yield testing of each of the fuels suggests that the optimal fuel composition contains 35% aluminum powder by mass.

15. SUBJECT TERMS
Hybrid Rocket, Paraffin, Aluminum Powder, Regression Rate, Rocketry, Rocket Science

16. SECURITY CLASSIFICATION OF:			**17. LIMITATION OF ABSTRACT**	**18. NUMBER OF PAGES**	**19a. NAME OF RESPONSIBLE PERSON**
a. REPORT	**b. ABSTRACT**	**c. THIS PAGE**		39	**19b. TELEPHONE NUMBER** *(include area code)*

U.S.N.A. --- Trident Scholar project report; no. 492 (2020)

OPTIMIZING THE STRUCTURAL AND DEFLAGRATION PROPERTIES OF ALUMINUM-RICH PARAFFIN-BASED HYBRID ROCKET MOTORS

by

Midshipman 1/C Kaden C. Dohm
United States Naval Academy
Annapolis, Maryland

_____
(signature)

_____
(date)

Certification of Adviser(s) Approval

Associate Professor Jin Kang
Aerospace Engineering Department

_____
(signature)

_____
(date)

Instructor of Practical Applications Spencer Temkin
Aerospace Engineering Department

_____
(signature)

_____
(date)

Acceptance for the Trident Scholar Committee
Professor Maria J. Schroeder
Associate Director of Midshipman Research

_____
(signature)

_____
(date)

USNA-1531-2

Abstract

Hybrid rocket motors offer an alternative to conventional solid motors and liquid engines. One of the most severe limiting factors of hybrid rocketry is the low regression rate as the fuel does not burn nearly as quickly as in a solid rocket. However, the discovery of liquefying fuels such as paraffin has greatly improved the regression rate of hybrid rocket fuels. Such fuels operate by liquefying to a greater extent than conventional fuels, whereby the low viscosity allows droplets of the fuel to become entrained in the oxidizer flow which increases the speed of the combustion process. Paraffin has a low compression strength and fractures easily. Recent studies show that the incorporation of polyethylene and aluminum powder can maintain and even increase the high regression rate of paraffin rocket motors, and increase the structural strength to allow these motors to survive the flight loads they experience during launch. This project seeks to further advance the benefits of the addition of aluminum powder as previous research suggests that the addition of aluminum powder at a concentration greater than 25% by mass could greatly increase the regression rate. As the concentration of aluminum powder increases more energy is released from the combustion of the fuel which increases the temperature of the combustion resulting in a faster regression rate, but the fuel also becomes more viscous which prevents the entrainment of fuel droplets which serves to limit the regression rate. Due to the COVID-19 pandemic test fires were unable to be completed to measure the regression rate of the fuel samples with a higher concentration of aluminum powder. However, data from compressive yield testing of each of the fuels suggests that the optimal fuel composition contains 35% aluminum powder by mass.

Keywords

Hybrid Rocket
Paraffin
Aluminum Powder
Regression Rate
Rocketry
Rocket Science

Table of Contents

Technical Nomenclature

DSC	Differential Scanning Calorimetry
HTPB	Hydroxyl-Terminated Polybutadiene
SEM	Scanning Electron Microscope
TGA	Thermogravimetric Analysis
a	Regression Rate Coefficient
A_t	Area of Nozzle Throat
A_2	Area of Nozzle Exit
B	Mass Transfer Number
C^*	Characteristic Velocity
D_{pf}	Final Grain Port Diameter
D_{pi}	Initial Grain Port Diameter
$\underline{G}$	Space-time Averaged Total Propellant Mass Flux
h_c	Heat of Flame Zone
h_g	Effective Heat of Gasification
h_w	Heat of Fuel Wall
I_{sp}	Specific Impulse
k	Ratio of Specific Heat Constants
$\frac{dm}{dt}$	Combustion Rate
$\dot{m}$	Total Mass Flow
$\dot{m}_{ent}$	Mass Entrainment Flow Rate
Δm_f	Mass Difference between Initial and Final of Fuel Grain
m_o	Time Averaged Oxidizer Mass Flow Rate
p	Dynamic Pressure
P_1	Pressure at Nozzle Inlet
P_2	Pressure at Nozzle Exit

$\dot{r}$	Regression Rate
t_b	Burning Time
t_{ig}	Ignition Time
t_{max}	Maximum Combustion Time
T_b	Burnout Temperature
T_d	Initial Decomposition Temperature
T_{ig}	Ignition Temperature
T_p	Peak Temperature
T_l	Temperature at Nozzle Inlet
u_c	Velocity of Propellant Gas down the Port at Flame
u_e	Velocity of Propellant Gas down the Port at the Boundary Layer Edge
X_c	Combustion Index
X_i	Ignition Index
δ	Melt Layer Thickness
μ	Viscosity
ρ_f	Fuel Density
σ	Surface Tension

Basic Rocketry Terminology

Various terms are defined in order to provide a fundamental understanding of some of the terminology that will be used throughout this report.

Regression Rate

The regression rate of a fuel refers to how quickly the grain port at the end of a rocket expands. In other words, it is defined by how quickly the radius of the hole at the end of the rocket increases as the rocket burns. Imagine looking at the bottom of a rocket. Figure 1 shows how the radius of the port expands as the rocket fires.

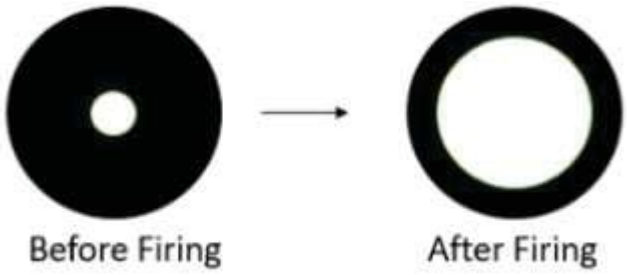

Figure 1: Depiction of the regression rate of a solid or hybrid rocket motor.

Thrust

Thrust is the name given to the force that is produced by rockets. By Newton's second law every action must have an equal and opposite reaction. This means that as a rocket generates hot gas that is ejected out of the nozzle, there must be an equal force that pushes the rocket in the opposite direction of the hot gases. This force is known as thrust.

Specific Impulse

Specific impulse is a standard measure of efficiency for rockets in the aerospace engineering discipline. It is calculated by dividing the total impulse delivered to the rocket by the mass that was used to achieve that impulse. In other words it tells an engineer how much fuel they will need to achieve a specified increase in velocity. It can be thought of as the mileage per gallon of a car.

Throttle

The term throttle is commonly used in many aspects of engineering and everyday life. When used in rocketry it means that the thrust that is produced by the rocket can be controlled by various mechanisms on the rocket. This means that firing can stop and start and that different levels of thrust can be achieved.

Oxidizer

In order for anything to burn it must have oxygen. Instead of using oxygen from the atmosphere to burn the fuel, most rockets carry oxidizers with them onboard. This allows a rocket to produce thrust in space where there is no oxygen available.

Fuel Grain

This is a term used to refer to the fuel in either a solid rocket or hybrid rocket.

List of Figures & Tables

1. Background

Hybrid rockets combine the designs of both liquid and solid rockets. These systems operate by storing the fuel in a solid state and the oxidizer in a liquid state at a location in which it can be easily pumped through the solid fuel. Historically, these systems have been rarely used in space launch vehicles because they are often unable to produce high levels of thrust due to their low regression rate and other inherent complexities. A basic schematic for a hybrid rocket engine is depicted in Figure 2.

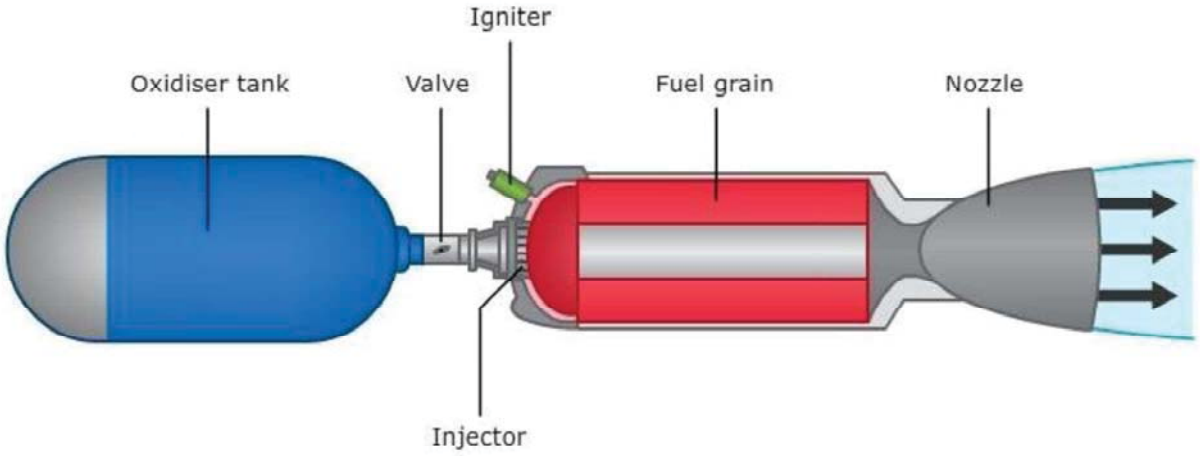

Figure 2: Basic design of a hybrid rocket engine [1].

In a liquid rocket, the fuel and oxidizer are able to intermix and fully combust in the combustion chamber of the rocket. This is why these rockets are so efficient. Solid rockets, on the other hand, contain both the oxidizer and the fuel in close proximity to each other in a solid state, so a simple spark can cause the fuel to combust very easily. Hybrid rockets, however, combust in a manner where the fuel becomes entrained by the oxidizer flowing past it before it deflagrates. This results in a much safer rocket system, but it also has a major impact on the regression rate of the fuel grain which leads to low levels of thrust and inefficiency.

2. Motivation

Separating the oxidizer and the fuel in a hybrid rocket system means the propulsion system is inherently much safer than conventional solid fuel rockets and some liquid fuel designs. This is because when catastrophic failures occur the oxidizer and the fuel have a much lower chance of combusting in a manner which would resemble an explosion. This poses a much safer design to personnel and equipment should a failure ever arise. Furthermore, hybrid rockets also have the potential for a higher I_{sp} than solid rocket engines. This is due to the fact that highly energetic materials such as aluminum can be added to the fuel mixture in much higher concentrations [2]. However, hybrid rocketry is often considered to be more of a novelty than a useful technology to

contemporary space launch vehicles and missile systems. Many problems are inherent in the design of hybrid rocket engines with the chief among these being the low regression rate of hybrid fuel grains which leads to limiting the amount of thrust that a hybrid rocket can produce.

Many solutions have been offered in recent literature to increase the regression rate of hybrid rocket grains with the addition of aluminum in a paraffin-based motor. One study by Hindustan University in India found that a fuel with 25% concentration of aluminum powder by mass yielded much stronger structural properties than a pure paraffin motor and had a nearly equitable regression rate [3]. Since this paper will be cited often and greatly influences this Trident project it is attached in *Appendix A.* However, this study seems to have stopped short in proving the potential of adding aluminum to a paraffin-based hybrid rocket motor as the structural and deflagration properties of the rocket grains continued to increase as the concentration of aluminum increased. The goal of this Trident Project is to continue to increase the concentration of aluminum in a paraffin-based hybrid rocket motor to find the point at which the regression rate is optimized. This will yield a much more powerful fuel composition that will help to solve the technical issues that modern hybrid rockets are facing. In doing so hybrid rockets will have a much greater potential for use in space launch vehicles and missiles and provide these systems with more efficient and safe propulsion.

3. Hybrid Rocket Combustion Theory

In order to better understand hybrid rocketry, it is best to begin by looking at combustion theory and internal ballistics. However, rocket internal ballistics is highly complicated and involves numerous physical processes which are extremely difficult to accurately model. Hybrid rockets burn much slower than solid rockets due to the separation of the oxidizer and fuel. In order for the solid fuel grain to burn it must first become entrained in the oxidizer flow before it can combust and generate thrust for the rocket. There are two main internal ballistic theories for hybrid rockets that explain this distinction and highlight the potential benefits of paraffin-based hybrid rockets. The first internal ballistic theory is the diffusion-limited combustion theory by which the majority of contemporary hybrid rockets operate. The second internal ballistic theory is the liquefying fuel combustion theory by which paraffin-based hybrid rockets are generally modelled.

3.1 Diffusion Limited Combustion Theory

Diffusion limited combustion theory applies to the vast majority of modern hybrid rocketry. This theory applies to hybrid rocket fuels that have high melting points, high viscosity, and high specific heat capacity such as Hydroxyl-terminated polybutadiene (HTPB). As the rocket combusts the fuel sublimes into a gas and diffuses away from the fuel surface. This diffusion of gasified fuel is what serves to severely limit conventional hybrid rocket fuels. Figure 3 depicts the internal ballistics of such a hybrid rocket.

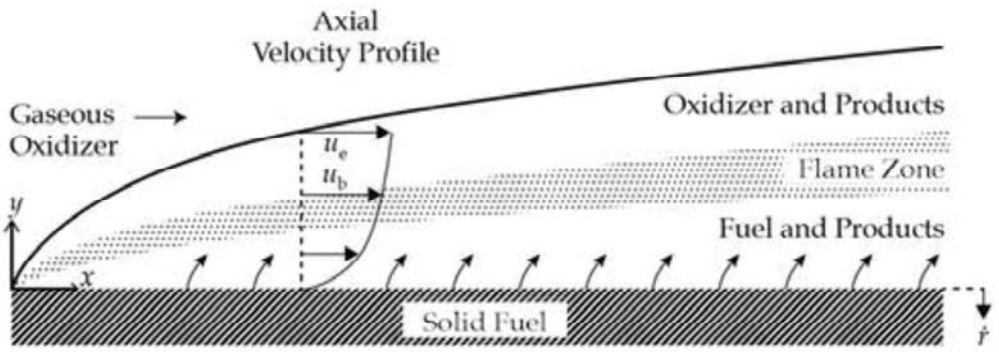

Figure 3: Diffusion-Limited Combustion Theory [4].

Since the fuel has a high melting temperature and a high viscosity, it is very difficult for the oxidizer flow to entrain the fuel as the hybrid rocket burns. Therefore, the regression rate of the hybrid rocket is detrimentally affected as only a limited amount of fuel is able to burn at a time. Furthermore, the high specific heat capacity of fuels such as HTPB means that the underlying fuel grains of the hybrid rocket does not heat up nearly as quickly as a fuel with a low specific heat capacity.

Overall, the diffusion-limited combustion theory depicts the issues inherent in hybrid rockets in that they do not allow nearly as much fuel and oxidizer to combust than in solid rockets or liquid rockets. This leads to a slow regression rate which greatly hinders the thrust and efficiency of hybrid rockets. However, recent advances in paraffin-based hybrid rockets are not accurately modeled by this theory.

3.2 Physical Processes in Diffusion-Limited Hybrid Rocket Combustion

Although diffusion-limited hybrid rockets can be basically understood by the simple narrative that the fuel sublimes, diffuses, then combusts by the oxidizer mass flow, there are actually many different physical processes inherent in the combustion of these hybrid rockets.

On the macroscopic level, the fuel has a temporally and spatially dependent gradient of velocities, temperatures, and species. Due to the friction of the surface of the fuel grain, the velocities of the oxidizer mass flow are significantly reduced due to the boundary layer. Furthermore, as the fuel combusts, the flame releases heat energy from convection and radiation. On the microscopic level, there is the potential for a thin surface melt layer depending on the type of fuel along with polymer chain breaking and reorganization, desorption of polymer fragments, and mechanical compression due to pressure differentials. These main physical processes are depicted in Figure 4 to provide a visual of the combustion process in diffusion-limited hybrid rockets.

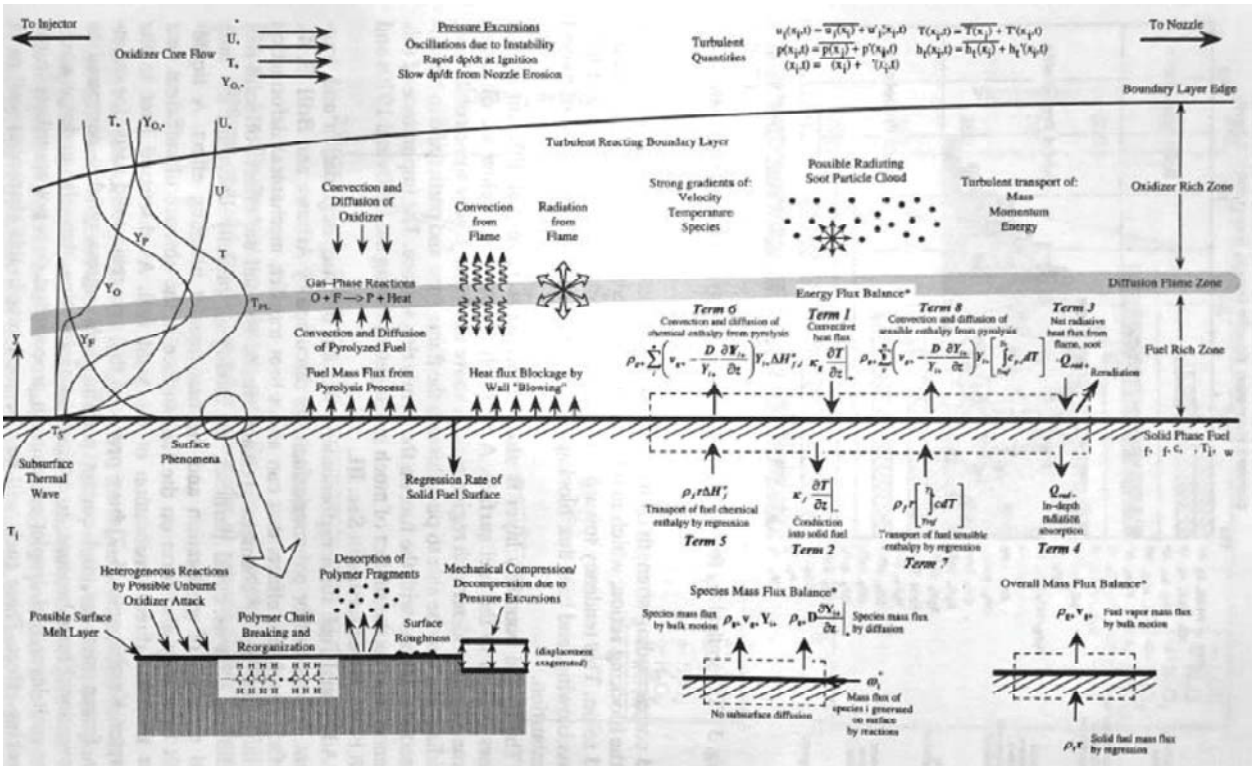

Figure 4: Physical Processes Involved in Diffusion-Limited Hybrid Rocket Combustion [5].

Although these physical processes are quite dynamic, these types of hybrid rockets can be modelled from their thermochemical properties. In the 1960s, Gerald Marxman and his colleagues modelled the diffusion-limited combustion process as shown in Figure 4, then they derived an energy balance with terms that include the conduction, convection, and radiative energy into and out of the fuel grain. In addition, there are a few other parameters to include the transport of fuel chemical enthalpy by regression and transport of fuel sensible enthalpy by regression. Marxman then assumed that the smallest of these terms were negligible and disregarded them in order to further simplify the energy balance and solve for the regression rate of the fuel grain.

The resulting regression rate equation is shown by Equation 1 and is related to the parameters $\underline{G}$, the total propellant mass flux, and B, the mass transfer number, which are calculated by Equation 2 and Equation 3 respectively [6].

$$\dot{r} = \frac{a}{\rho_f} G^{0.75} B^{0.23} \tag{1}$$

$$\underline{G} = \frac{16(m_o t_b + \Delta m_f)}{\pi(D_{pi} + D_{pf})^2 t_b} \tag{2}$$

$$B = (\frac{u_e}{u_c})(\frac{h_c - h_w}{h_g}) \tag{3}$$

Equation 2 represents the total propellant mass flux. These parameters are the fuel mass differential, Δm_f, the oxidizer mass flow rate, m_o, and the port diameters, D_{pi} and D_{pf}. Furthermore, the ratio of the gas propellant velocity at the boundary layer to its velocity at the flame ($\frac{u_e}{u_c}$) can be explained by the relationship in Equation 4

$$\frac{u_e}{u_c} = \frac{1 + (\frac{O}{F} + 1)(\frac{h_c - h_w}{h_g})}{\frac{O}{F}(\frac{h_c - h_w}{h_g})} \tag{4}$$

where $\frac{O}{F}$ is the oxidizer to fuel ratio, the heat of the fuel wall is h_w, the heat of combustion is h_c, and the heat of gasification is h_g. The derivation process for Marxman's regression rate model is provided in more depth by M. Chiaverini and K. Kuo[5].

While this model can be used to accurately model standard diffusion-limited hybrid rocket fuels such as HTPB, it begins to break down due to the introduction of a new and significant physical process. With the advent of paraffin-based rockets, new fuels were discovered that not only diffuse but also entrain fuel droplets in the oxidizer flow to an extent that is no longer negligible.

3.3 Liquefying Fuel Combustion Theory

Paraffin-based hybrid rockets have a low melting temperature, a low viscosity, and a lower specific heat capacity than most diffusion-limited hybrid rocket fuels. This allows much more of the rocket fuel to become entrained in the oxidizer flow which increases the regression rate and the potential amount of thrust that can be generated. Figure 5 depicts this behavior in the liquefying-fuel combustion theory.

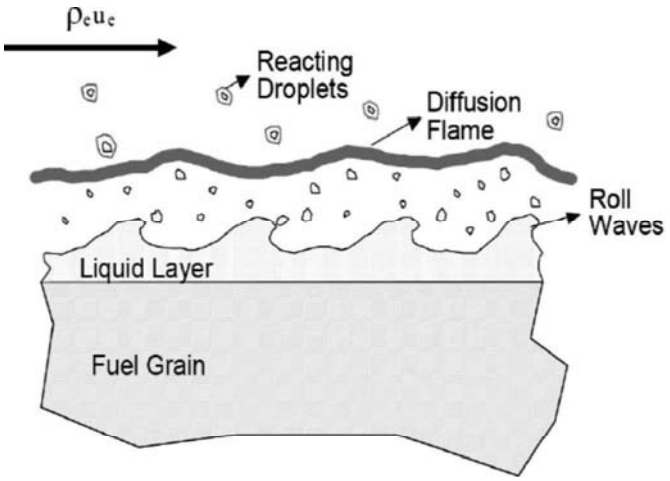

Figure 5: Liquefying Fuel Combustion Theory [7].

As the rocket fuel combusts, the heat generated melts the fuel grain to form a thick liquid layer. This liquid layer has a very low viscosity, which means that the oxidizer mass flow is able to entrain droplets of the liquid fuel as it flows. Furthermore, the fuel is able to transfer heat very well to the underlying fuel grain due to its low specific heat capacity. This means that the liquid layer will increase in thickness and more droplets of the fuel can become entrained. Due to the lower melting temperature, low viscosity, and the low specific heat capacity, more of the fuel is able to interact with more of the oxidizer which means that it is able to combust more quickly and generate higher levels of thrust.

Equation 5 describes the relationship between the entrained mass flow rate and the dynamic pressure, melt layer thickness, surface tension, and viscosity of the fuel grain

$$\dot{m}_{ent} \propto \frac{P^{a}\delta^{\beta}}{\sigma^{\pi}\mu^{c}} \tag{5}$$

where P is dynamic pressure, δ is the melt layer thickness, σ is the surface tension, μ is the viscosity, and the exponents $a, \beta, \pi,$ and c are experimentally derived and are used to more adequately fit the model to the data. This equation helps to qualitatively understand what factors lead to an increase in the regression rate although it is not used quantitatively to determine, calculate, or predict the regression rate as properties involved are dynamic throughout the firing of the motor.

3.4 Empirical Model of Entrainment Regression Rate

While the vast majority of effort focuses on modeling diffusion-limited hybrid rocket internal combustion, a few studies have attempted to model the liquefying fuel combustion theory in

order to ascertain the amount of liquid entrainment that occurs in these types of hybrid rockets. A study published by the American Institute of Aeronautics and Astronautics (AIAA) details a model that accurately determines the entrainment regression rate of liquefying fuels by using Marxman's model to calculate the diffusion-limited regression rate from the thermochemical properties of the fuel, then test fires a rocket motor to measure the total combustion rate. When the vaporization regression rate that is calculated is subtracted from the total regression rate that is measured from the experimentation, the entrainment regression rate can be determined [6].

According to S.Kim, J. Lee, and H. Moon, entrainment accounts for roughly 70% of the total regression rate for pure paraffin hybrid rocket motors. This value decreases to approximately 20% with the addition of 10% polyethylene into the fuel composition by mass [6].

3.5 Aluminum Powder Addition Theory

Aluminum in a fine powder form is extremely combustible, releases high amounts of energy, and has an even lower specific heat capacity than paraffin. These three properties mean that with the addition of aluminum powder to a paraffin-based hybrid rocket motor, the regression rate will increase. Furthermore, aluminum powder greatly increases the structural properties of hybrid rockets which allows them to handle the flight loads placed on the rocket during a launch. However, as the concentration of aluminum powder increases in a paraffin-based hybrid rocket motor, the ratio of the polyethylene to the paraffin increases which thereby causes the viscosity and surface tension of the fuel to greatly increase. Research conducted by Hindustan University shows that although aluminum powder by itself does not increase the viscosity of the fuel, the increased ratio of polyethylene to paraffin will increase it [3].

As described in Equation 1, as the concentration of aluminum powder increases, the heat released by the fuel as it burns will increase which will increase the temperature of the motor thereby increasing the dynamic pressure and the melt layer thickness. However, with the increased concentration of aluminum powder also comes an increase in the surface tension and the viscosity of the liquid layer of the fuel which will serve to limit the regression rate of the fuel grain.

There is an optimum concentration of aluminum powder where the melt layer thickness and dynamic pressure will increase to the greatest extent while at the same time minimizing the increase in the surface tension and viscosity of the fuel. Figure 6 depicts the overarching trends in the properties of the fuel as the concentration of aluminum powder increases.

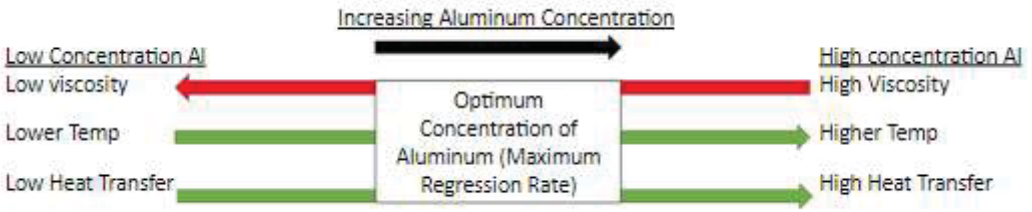

Figure 6: Strategic depiction of the effect of increased aluminum powder on fuel properties.

Hindustan University conducted tests on paraffin-based hybrid rocket motors with the addition of 10% polyethylene powder and varying concentrations of aluminum powder from 0% to 25% by mass. Polyethylene was added in order to enhance the structural properties of the fuel and to limit the expansion of the paraffin when heated during casting. It was determined that the regression rate of the 25% aluminum powder sample was the highest of any of the samples with aluminum powder. Therefore, the optimum concentration of aluminum powder is likely above 25% as the regression rate continued to increase as the concentration of aluminum powder increased [3].

3.6 Inability to Apply Entrainment Regression Rate to Fuels With Additives

Diffusion-limited hybrid rockets have long been used in the aerospace industry, and models to predict their regression rate exist with reasonable accuracy. In recent years, studies have been published that attempt to model the behavior of liquefying fuel hybrid rocket motors, but typically these studies rely upon experimental test fires in order to ascertain the regression rate from the entrainment of the fuel droplets.

There does not exist a model that can accurately predict the regression rate of a liquefying fuel hybrid rocket solely from its thermochemical properties. Furthermore, with the addition of aluminum powder into the fuel composition, a new physical process is introduced in which the fine aluminum particles ablate from the surface of the fuel. Due to the inherent complexity and dynamic nature of aluminum powder ablation and liquefying fuel combustion theory, models alone cannot be used to determine the regression rate of these hybrid rocket fuels. Experimental test fires must be conducted in order to gain conclusive results for the regression rates.

4. Methodology

In order to determine the structural and thermochemical properties of the fuel compositions, there are four main processes involved in this project. The first is the synthesis of fuel coupon samples for compression testing and rocket motors for experimental test firing. The second is the testing of structural properties of the fuels to ensure that they can handle the loads placed on them during a rocket launch. The third is the testing of combustion properties to gain a deeper

insight into the internal combustion while the rocket is firing. The final process is the experimental test firing to determine the regression rate.

4.1 Synthesis of Hybrid Rocket Grains

4.1.1 Material Selection

Three main materials were used in the hybrid rocket fuel samples: paraffin, polyethylene, and aluminum powder. Table 1 lists key properties and identifying information for these three materials so that future testing can be replicated with similar results. These materials were selected to be as similar to those that were used by Hindustan University in order to cross check various results [3].

Table 1: Key properties and identifying information for materials used in sample synthesis.

Material	Supplier	Product No.	Density	Melting Point (°C)	Particle Size (µm)
Paraffin	Supelco	1071511000	0.90 g/ml	42-72	n/a
Polyethylene	Sigma Aldrich	428078	0.918 g/ml	100-125	n/a
Al Powder	Supelco	1010560250	26.98 g/mol	660	20-100

4.1.2 Fuel Coupon Synthesis Process

To test small samples of rocket fuel, small coupon samples were manufactured. In order to cast the sample, a split mold was 3-D printed by the machine shop at the United States Naval Academy. The mold was created to generate a sample that would be a cylinder with a 2 cm diameter and 3 cm in height. These samples could then be used for compression testing and all other forms of testing. Figure 7 depicts the split mold that was created by the machine shop. It is held together by four screws with wing nuts. Honey Wax, a grease removal agent, was also coated to the walls of the split mold in order to easily remove the cooled sample.

Figure 7: An image of the split mold created for sample synthesis.

Hindustan University details in-depth how they synthesized hybrid rocket fuels. The process involved melting a premeasured amount of paraffin in a beaker on a hot plate, adding the polyethylene and allowing it to melt and mix with the paraffin over 30 min, adding the aluminum powder, then placing the homogeneous mixture into a mold and allowing it to cool [3].

The same procedure was followed for the synthesis of the hybrid rocket fuel samples in this project. An analytical balance which has precision to the hundredths place for mass in grams was used to measure the mass of the paraffin, polyethylene, and aluminum powder. The hot plate was initially set to 200 °C while the paraffin was melted in the beaker. A magnetic stirring rod was added to the beaker and set to 300 rpm to stir the mixture. The polyethylene was added to the paraffin at the same temperature initially. Figure 8 shows the beaker with the magnetic stirring rod on the hot plate melting the polyethylene beads into the paraffin.

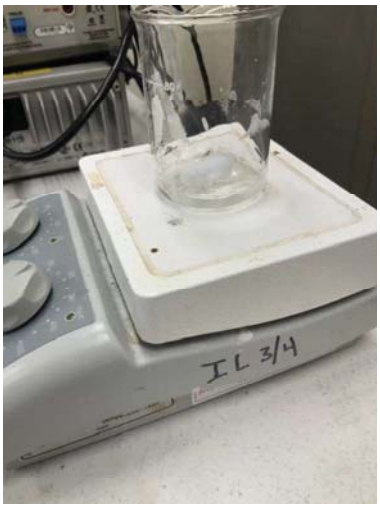

Figure 8: Image of polyethylene melting into paraffin while being stirred magnetically.

After ten minutes the temperature was increased to 300 °C and the magnetic stirring rod was slowly increased in angular rate as the polyethylene melted. The mixture becomes more viscous as the polyethylene melts and eventually the magnetic stirring rod is no longer able to generate enough torque to stir the material. Two spatulas were used to stir the material in the beaker as it was heated by the hot plate. As polyethylene would stick to one of the spatulas, the other would be used to scrape it off in order to keep dispersing the polyethylene homogeneously. Once the sample had become a uniform paste, the premeasured aluminum powder was added and stirred until it was spread evenly throughout the mixture.

Once the sample was melted and completely uniform in the beaker, it was ready to be cast. The split mold that was made by the machine shop was greased with Honey Wax, a grease removal agent, in order to easily remove the fuel sample from the mold after it had completely cooled. Once the sample was allowed to cool for a period of no less than two hours, it was ready to be removed. The wing nuts were removed from the screws, and two screwdrivers were used to pry the split mold apart. The sample was then easily removed from the split mold for testing. Figure 9 shows a sample in the split mold after it was removed.

Figure 9: Image of a sample removed from the split mold.

4.1.3 Fuel Compositions Tested

Hindustan University tested six different combinations of hybrid rocket fuels with paraffin, polyethylene, and aluminum powder. Table 2 displays the concentrations that were used in their testing. Since the structural and combustion properties of the fuels continued to improve with the addition of aluminum, higher concentrations of aluminum were tested in this project in order to ensure that the concentration of the aluminum in the fuel is optimized. However, a few of the same compositions were also tested in order to cross-check results and ensure continuity. Table 3 lists the concentrations that were tested in this research. The project proposal listed compositions up to 50% aluminum powder by mass, but after various synthesis attempts it was determined by

inspection that aluminum powder concentrations that high result in structurally unsound fuel samples that fracture easily. Therefore, the maximum aluminum powder concentration by mass was reduced to 40%.

Table 2: Compositions of previously tested paraffin-based fuels by Hindustan University [2].

Fuel Sample	Composition
Pure Paraffin	Paraffin 100%
P/PE05	Paraffin 95% + Polyethylene 5%
P/PE10	Paraffin 90% + Polyethylene 10%
P/PE/Al5	Paraffin 85% + Polyethylene 10% + Aluminum 5%
P/PE/Al15	Paraffin 75% + Polyethylene 10% + Aluminum 15%
P/PE/Al25	Paraffin 65% + Polyethylene 10% + Aluminum 25%

Table 3: Compositions of paraffin-based fuels tested in this project.

Fuel Sample	Composition
Pure Paraffin	Paraffin 100%
P/PE10	Paraffin 90% + Polyethylene 10%
P/PE/Al25	Paraffin 65% + Polyethylene 10% + Aluminum 25%
P/PE/Al30	Paraffin 60% + Polyethylene 10% + Aluminum 30%
P/PE/Al35	Paraffin 55% + Polyethylene 10% + Aluminum 35%
P/PE/Al40	Paraffin 50% + Polyethylene 10% + Aluminum 40%

4.1.4 Rocket Motor Synthesis Process

In order to experimentally determine the regression rate of the fuels, rocket motors of each composition had to be manufactured. This process had to be simple, regimented, and repeatable in order to obtain accurate data. To mitigate the potential for a failed test fire, more rockets would be manufactured than would be needed to obtain meaningful results. Four motors were planned to be manufactured for each of the six compositions resulting in a total of 24 rocket motors to be manufactured.

[These motors were not able to be manufactured due to the COVID-19 pandemic; however, in order to facilitate future work this process is still described.]

The process that was used to prepare the molten fuel as described in Section 4.1.2 would be followed in the same manner; however, a few new steps would be added in order to ensure that the prepared motors would be of the utmost quality. All of the new equipment that was going to be used is depicted in Figure 10.

Figure 10: Images of each of the materials to be used in the rocket motor synthesis [7][8][9].

Instead of pouring the molten fuel into a split mold, the fuel would be poured into a metal syringe that was wrapped with heat tape. The heat tape would keep the fuel from solidifying so that it could be pressed through the thin nozzle of the syringe. This process was added in order to remove air bubbles that could be present from pouring the mixture directly into the mold. The presence of air bubbles in a rocket motor leads to combustion instability that can invalidate results or cause damage to the test stand. The syringe would push the fuel into a paper phenolic tube that has a 2.54 cm inner diameter and 2.70 cm outer diameter. Furthermore, the rocket motors would all be cut to 13.97 cm in length. Paper phenolic is a composite material that is a strengthened version of high density cardboard. It is widely used for small scale rocket motors because it does not burn, but rather chars after all of the fuel has burned.

After the fuel was injected from the syringe into the paper phenolic tube, the motor would then be placed into a bell chamber and pumped to a near vacuum in order to allow more of the potential air bubbles to escape. The motor would then be allowed to cool for roughly two hours. After the rocket motor was properly cooled, a lathe would be used to cut out the port in the center of the motor to the proper dimension.

4.2 Testing Properties

4.2.1 Mechanical Properties

Two main tests were used to gather information about the structural and mechanical properties of the samples. In order to qualitatively depict the structure of the fuel grains, a scanning electron microscope was also used to capture images of samples. To quantitatively determine the increase in strength of the fuel samples, compression yield testing was conducted.

4.2.1.1 Compressive Yield Testing

Compressive yield testing is useful in providing quantitative data to depict the structural strength of the fuel samples. When a hybrid rocket is being launched, it will experience compressive flight loads acting on it which it must sustain in order to maintain structural rigidity and consistent burning. Three samples of each of the six fuel compositions were tested in order to

cross-check the results. The resulting compressive yield strength and compressive Young's Modulus were averaged.

The rocket fuel samples were placed onto a load frame and then compressed at a constant rate of 0.004 in/s. The corresponding pressure measured by the load frame was then measured at each time step. The pressure could then be plotted against displacement in order to determine the compressive yield point and the compressive Young's Modulus. Figure 11 shows the load frame that was used in the experimentation with a sample loaded into the test cell.

Figure 11: Image of the load frame used for testing with a sample in the test cell.

The compressive yield point is the point at which the fuel grain is no longer able to support the compressive force without yielding and losing its shape. The compressive Young's Modulus measures how well the fuel grain is able to maintain its shape while compressive stress is acting upon it. For the fuel samples, a high compressive yield point and compressive Young's Modulus is desired. Furthermore, the failure modes of the fuels were observed. A ductile failure mode is observed when the fuel is able to maintain its shape without fracturing during the test. If fracturing occurs, then the fuel samples experience a brittle failure mode which is much less desirable.

4.2.1.2 Scanning Electron Microscope Imaging

A scanning electron microscope (SEM) operates by shooting a beam of electrons at an object and then measuring the reflected electrons in order to generate an image. Aluminum has a high conductivity, and, therefore, easily reflects electrons back at the detector. Paraffin and polyethylene, on the other hand, absorb electrons. Aluminum will appear bright on the SEM

images and paraffin and polyethylene will appear dark. By taking SEM images, the dispersion of the aluminum powder in the samples can be more easily depicted in order to better understand how it affects the structural properties of the fuel grains. This will be key to understanding why certain fuel samples exhibit better structural properties than others. However, since the paraffin and polyethylene both absorb electrons, they appear to be nearly the same material under the scanning electron microscope which makes it difficult to ascertain whether the polyethylene is being evenly dispersed in the paraffin.

4.2.1.3 Rheometry

Rheometry measures the viscosity of samples. It is affected by both temperature and shear speed. The testing operates by placing a material on a test bed, then a cylindrical mechanism is lowered on top of the sample. As the cylinder rotates, the torque and the angular displacement are measured in order to calculate the viscosity of the sample. Various geometries are available to test the viscosity of fuel samples. For the pure paraffin and PP/PE samples, 60 mm parallel steel plates were used to run the rheometry experiments.

The test cycle for the pure paraffin sample measured the viscosity at temperatures ranging from 60 to 100℃ and shear rates from 1 to 100 Hz. The PP/PE10 sample was measured at temperatures ranging from 120 to 150℃. This sample was tested at higher temperatures in order to ensure that all of the polyethylene was liquidated. The paraffin sample was not tested at this same temperature in order to prevent decomposition of the paraffin.

Due to the presence of aluminum powder in the other four samples, data that was collected with the parallel plates yielded no valuable data; therefore, a concentric cylinder geometry had to be used, but required more material than was available.

[More samples were going to be prepared following spring break, but due to the COVID-19 pandemic, rheometric data was only collected for the pure paraffin sample and PP/PE10 sample.]

4.2.2 Thermochemical Properties

4.2.2.1 Thermogravimetric Analysis (TGA)

Thermogravimetric analysis (TGA) operates by monitoring the mass of a substance as the temperature is increased at a constant rate. This allows various properties to be determined about the material to characterize how the materials ignite, decompose, and combust as the rocket grains burn. Although TGA cannot be used to directly predict the regression rate of hybrid rocket fuels, it still provides valuable data on the underlying thermochemical properties.

RTI Laboratories in Livonia, MI, was contracted to run TGA in an oxygen environment to observe combustion properties and in nitrogen to observe pyrolysis properties. For each test a sample of 5 to 10 mg was placed in a platinum dish and tested for its thermal profile. The sample started at room temperature and was increased 10°C/min to 800°C.

Two main categories of properties were derived from the thermal profile: ignition properties and combustion properties. The initial decomposition temperature, T_d, is defined as the temperature which corresponds to when 0.1% of the mass has decomposed on the pyrolysis thermal curve. It indicates the start of the decomposition process. The ignition temperature, T_{ig}, corresponds to when 0.1% of the mass has combusted on the thermal curve from the TGA analysis in an oxygen environment. The ignition time, t_{ig}, also corresponds to this same point.

One of the most significant combustion properties is the max combustion rate, $\frac{dm}{dt}_{max}$, which corresponds to the fastest decrease in mass on the thermal curve. The peak temperature, T_p, and the max combustion time, t_{max}, both correspond to this point. The burnout temperature, T_b, and the burnout time, t_b, both correspond to the point where the thermal curve plateaus and combustion ceases to occur.

Hindustan University further developed arbitrary equations known as the ignition index, X_i, and the combustion index, X_c. These two equations serve as a basis to compare the ease of ignition of the fuel and the speed of combustion, respectively. Equation 6 describes the relationship for the ignition index and Equation 7 describes the relationship for the combustion index [3].

$$X_i = \frac{(\frac{dm}{dt})max}{t_{max} \cdot t_i} \tag{6}$$

$$X_c = \frac{(\frac{dm}{dt})max(\frac{dm}{dt})avg}{{T_{ig}}^2 \cdot T_b} \tag{7}$$

4.2.2.2 Differential Scanning Calorimetry (DSC)

Differential scanning calorimetry (DSC) operates similarly to TGA; however, instead of determining how the mass changes as a result of a steady constant increase in temperature this thermal analysis technique monitors how the material's heat capacity is changed by temperature especially during phase changes. This allows other important parameters of the fuel to be determined, most particularly the melting point of the various materials within the fuel (i.e. paraffin, polyethylene, and aluminum powder), and the net endothermicity and net exothermicity which shows how energy is transferred during the heating process.

RTI Laboratories once again conducted the DSC testing. A sample of 5 to 10 mg was loaded onto a platinum dish and tested. The sample started at room temperature and was raised 10°C/min to 300°C. From this data the melting points of the material involved can be gleaned from spikes in the thermal curve.

4.3 Hybrid Rocket Test Firing

4.3.1 Test Setup

In order to gather experimental data for the regression rate and the characteristic velocity of the rocket motors, the motors were going to be test fired at Penn State University. [However, due to the COVID-19 pandemic, the testing was not able to be completed.] The test stand is equipped to fire hybrid rocket motors that are at a maximum of 1 in diameter due to the size of the combustion chamber. This test stand houses the rocket motor and the nozzle inside of a retainer system that is then connected to the gaseous oxygen tank. Liquid oxygen is the same oxidizer that was used by Hindustan University in their test fires, and was selected due to its availability and wide use in the field. Figure 12 displays the various components that are included in the test stand.

There are many parameters that must be properly controlled in order to ensure a successful test fire. These parameters include the chamber pressure which is controlled by the throat size of the nozzle and the oxidizer mass flow rate. Furthermore, the most accurate data comes from a smooth and consistent burn, so it would be critically important to ensure that the rocket motors were manufactured with no inconsistencies, air pockets, or deficiencies. Nozzles serve to expand and accelerate the flow of the hot gases that are expelled from a rocket fire. In order to maintain a constant chamber pressure between test firings, which would allow for the greatest basis for comparison, the throat area of the nozzles had to be calculated from the hypothesized regression rate of the fuel. Figure 13 depicts a model of a nozzle.

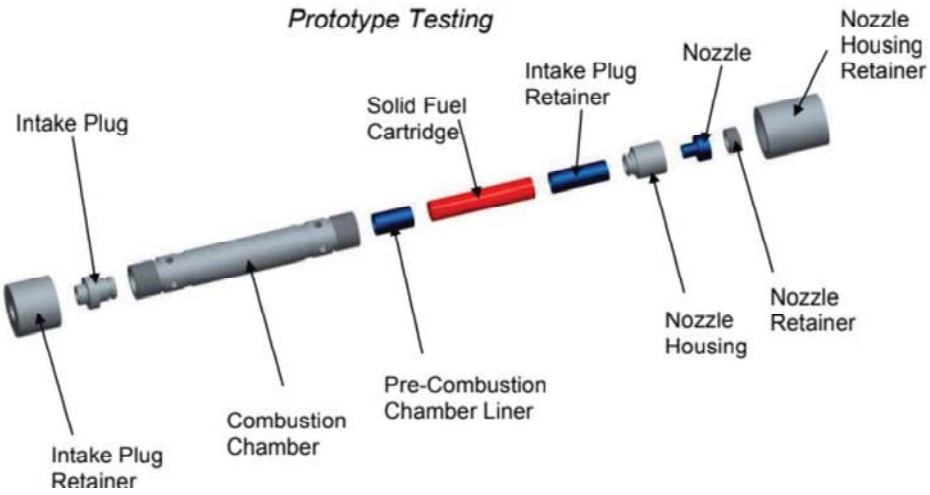

Figure 12: Visual depiction of the components in the test stand.

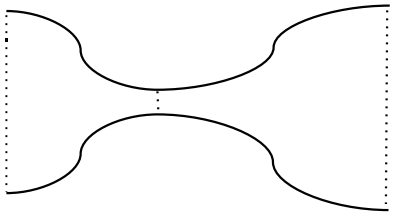

Figure 13: Model of a nozzle. Area 1 refers to the chamber and area 2 refers to the nozzle exit.

Equation 8 is used to calculate the throat area of the nozzle in order to "choke" the flow, or force the flow at the throat to become sonic

$$A_t = \frac{\dot{m}}{P_1}\sqrt{\frac{RT_1}{k[2/(k+1)]^{(k+1)/(k-1)}}} \tag{8}$$

where $\dot{m}$ is the total mass flow rate, which can be calculated from the regression rate of the fuel, P_1 is the desired chamber pressure, R is the specific gas constant, and k is the ratio of specific heat capacities.

Nozzles were to be manufactured by the USNA machine shop from graphite rods. Graphite was the material selected due to its high thermal resistance; however, this comes at the cost of durability as the nozzle's throat would ablate to a point of no longer being usable after about three or four test fires. Therefore, multiple nozzles were to be manufactured. In order to conduct the test fire, the motor and nozzle would be placed into the housing and screwed shut. Based upon the hypothesized regression rate of the fuel, the oxidizer would only flow for a limited period of time, so that the paper phenolic casing would not burn. Once the housing was properly reassembled, it would be connected to the gaseous oxygen tank. The oxidizer flow valve would

then be released to allow the liquid oxygen to flow before the igniter is sparked by the computer control system. The computer then shuts off the oxidizer flow and purges the test cell with nitrogen to extinguish all flames.

4.3.2 Regression Rate Determination

As the rocket motor fires, the grain port will regress unevenly due to turbulent flow and boundary layers in the oxidizer flux. Therefore, measuring the final grain port diameter requires a more in depth procedure than simply measuring it with calipers. Figure 14 depicts the rocket motor with the port before and after the test fire.

Figure 14: Visual depiction of the rocket motor with port before and after firing. Uneven burning results in difficulty of measuring final grain port diameter.

In order to determine the grain port diameter, a flat piece of waterproof material will be epoxied to the base of the motor. The motor along with the attached material will then be weighed and recorded. Water is then added to the port and filled to the very top so that all of the volume inside the rocket motor is full. The motor with the water is then weighed and the difference between the two masses is determined to find the mass of water that occupies the volume in the motor. Using the density of water and the equation for the area of a cylinder, the final port diameter, d_f, can be determined. The regression rate is then calculated as the difference between the initial and final port diameter divided by the burn time.

4.3.3 Characteristic Velocity Determination

Characteristic velocity is a measure of the combustion performance of a rocket fuel and can be used as a basis of comparison for various hybrid rocket fuels. This parameter is very important in the determination of the feasibility of the motor to generate high levels of thrust. Regression rate is a key property of a rocket fuel that accounts for how quickly the fuel is able to burn, but in a liquefying fuel rocket motor the entrained droplets may not combust fully while in the combustion chamber which would lead to inefficiency. Characteristic velocity takes this downfall into account in order to gain a better basis of comparison for the ability of these rocket fuel compositions to generate high levels of thrust. Characteristic velocity is calculated by Equation 10

$$C^* = \frac{P_l A_t}{\dot{m}} \tag{10}$$

where P_l is the pressure in the combustion chamber, A_t is the throat area, and $\dot{m}$ is the total mass flow rate. After testing has been completed and the regression rate is calculated, the characteristic velocity can be calculated from the pressure that is recorded during testing, the known throat area of the nozzle, and the total mass flow which can be calculated from the regression rate and known oxidizer flow rate.

5. Results and Discussion

5.1 Mechanical Properties

5.1.1 Compressive Yield Testing

The compressive yield test for the six samples provided some interesting insight into the role that aluminum powder plays in the structural properties for the fuel grains. Figure 15 depicts the compressive yield test for the six samples. Each sample has a linear region that increases at a steep slope that corresponds to the Young's Modulus. The point at which the curve rounds off corresponds to the compressive yield point.

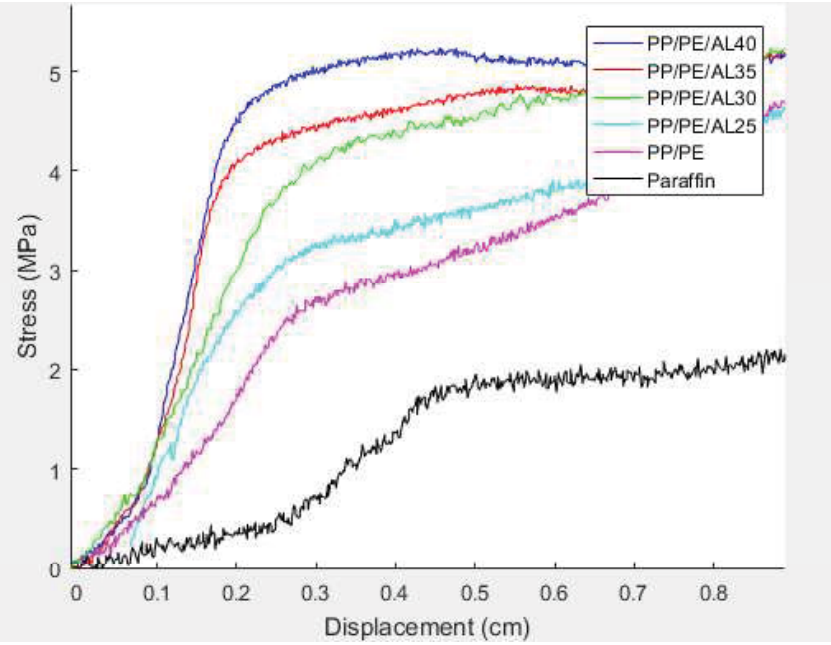

Figure 15: Compressive Yield Test for the six fuel samples.

In order to more accurately determine the structural properties of the fuel samples, the compressive yield force and the compressive Young's Modulus were calculated and compiled into Table 4.

Table 4: Compilation of the structural properties of the fuel samples derived from the compression testing.

Sample	Average Compressive Yield Point (MPa)	Average Compressive Young's Modulus (MPa)	Failure Mode
PP	1.26	16.8	Ductile
PP/PE10	2.05	25.2	Ductile
PP/PE/AL25	3.07	33.0	Ductile
PP/PE/AL30	3.88	37.4	Ductile
PP/PE/AL35	4.07	72.4	Ductile
PP/PE/AL40	4.77	73.0	Brittle

It is a noticeable trend in Figure 15 and Table 4 that as the concentration of aluminum powder increases, the compressive yield point and compressive Young's Modulus increase. The addition of aluminum powder decreases the size of the grains as the paraffin and polyethylene mixture cool, resulting in a stronger material that is capable of withstanding more compressive force.

One of the most significant observations made was the failure mode transition from ductile to brittle with the PP/PE/AL40 sample. All three of the samples for this composition fractured during the compression test. Even though this composition displays greater compressive yield strength than the other samples with less aluminum powder, the brittle failure mode is highly undesirable as potential stress concentrations from casting the motor could result in fractures in the fuel during a launch, which would result in catastrophic failure. Therefore, the sample that displays the most desirable structural properties is PP/PE/AL35.

5.1.2 Scanning Electron Microscope Imaging

SEM images were collected to get an insight into the structure and composition of the fuel grains. The most important qualities that were determined from the images were the determination of the size and shape of the grains and the distribution and homogeneity of the aluminum powder in the fuel samples.

Paraffin is a wax-like material that forms into grains when it cools after being melted and cast into shapes. The resulting structure generates large boundaries that can easily slip past each other when a load is placed on them. With the addition of polyethylene to paraffin, the grains decrease drastically in size and have more complicated shapes than pure paraffin. This means that it is more difficult for the grains to slip past others resulting in a stronger structure. Figure 16 shows this trend in SEM images that were taken by Hindustan University of pure paraffin and paraffin with 10% polyethylene by mass.

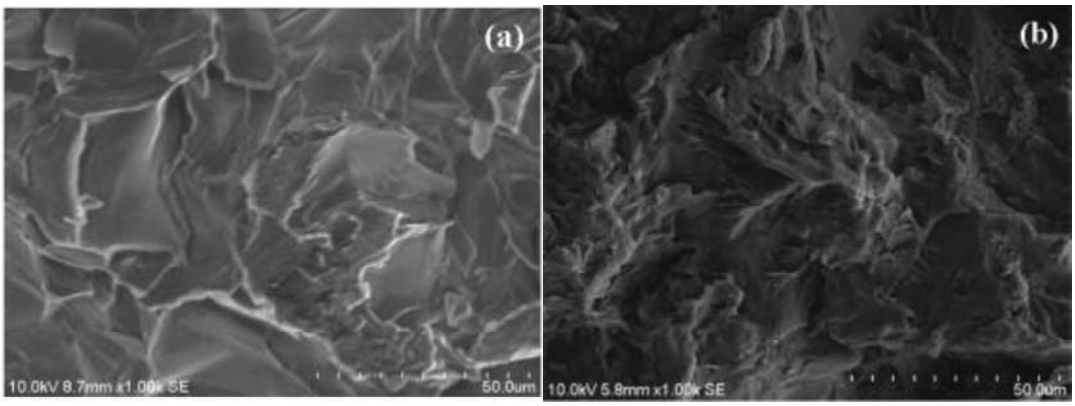

Figure 16: SEM of (a) paraffin and (b) paraffin with 10% polyethylene [3].

Aluminum powder is added to the paraffin and polyethylene mixture in order to both improve regression rate and structural properties. Figure 17 shows an SEM image of the aluminum powder. One of the most critical observations of the aluminum is that the flecks look more like flat shavings. The SEM was also tilted to capture an image at a 45° angle to confirm this hypothesis. The powder also ranges in size from 20 µm to 100 µm.

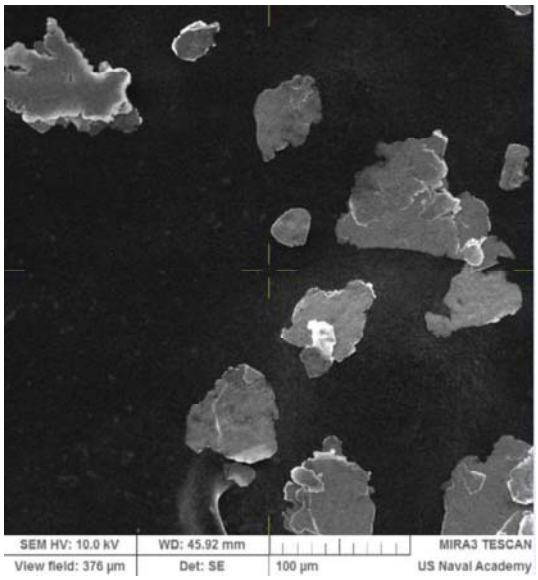

Figure 17: SEM image of aluminum powder.

The fuel samples with aluminum powder were also imaged in order to view the dispersion of the aluminum powder in the fuel. Figure 18 shows the four samples that include aluminum powder ranging in concentration from 25% to 40% by mass. The view field of each image is 1.66 mm and was captured with a 10 kV beam.

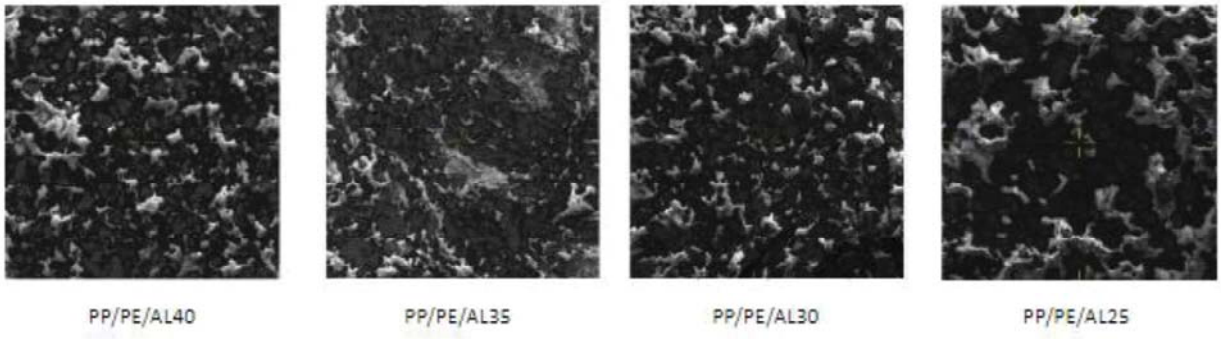

Figure 18: SEM images of fuel samples with aluminum powder.

One of the key trends that can be seen is that the aluminum powder disperses itself in veins throughout the paraffin and polyethylene mixture. The veins vary in shape and size and increase the ability of the fuels to handle stress as the concentration of aluminum powder increases. This is the same type of relationship that can be found in steels between the grain size and the strength of the steel.

5.1.3 Rheometry

The viscosity of pure paraffin and PP/PE10 was studied for various temperature and shear rate ranges. Figure 19 shows the viscosity measurements for pure paraffin for temperatures ranging from 60 to 100°C and shear rates ranging from 10 to 100 Hz. Data in the range of 1 to 10 Hz was sporadic as the steel plates were not able to maintain full contact with the sample during the test cycle as such low rotational speeds.

The viscosity of paraffin at 100°C with a shear rate of 10 Hz is 2.22×10^{-3} Pa·s. After a shear rate of 10 Hz, the paraffin begins to exhibit a more constant viscosity and exhibits the characteristics of a Newtonian fluid. Figure 20 shows the viscosity for PP/PE10 with a temperature range of 120 to 150°C with shear rates from 1 to 100 Hz.

For PP/PE10, the viscosity at shear rate of 10 Hz and temperature of 120°C is 1.06 Pa·s. Polyethylene is a long chained polymer that greatly increases the viscosity of the fuel. As can be seen, the viscosity of paraffin with and without polyethylene are orders of magnitude in difference. Another interesting trend is the non-Newtonian shear thinning that PP/PE10 displays for higher shear rates.

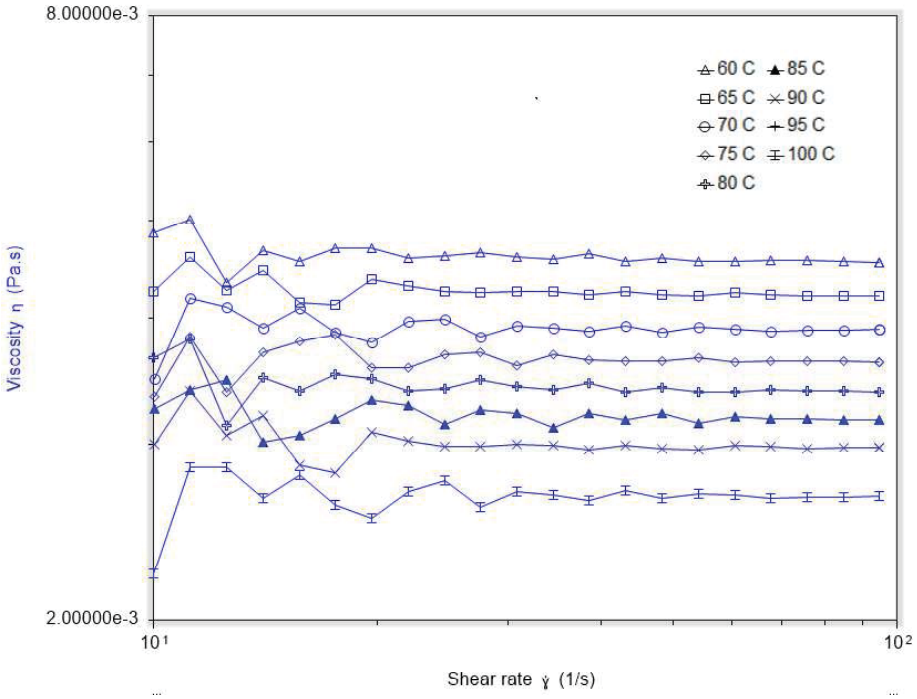

Figure 19: Graph of viscosity for pure paraffin with a temperature range of 60 to 100℃ and shear rates from 10 to 100 hz.

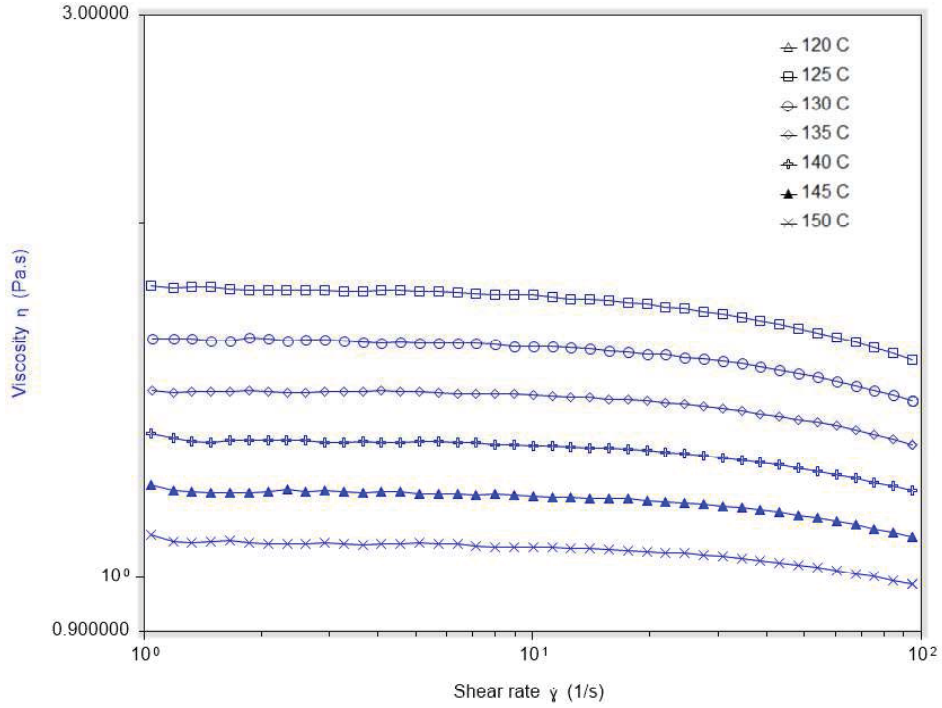

Figure 20: Graph of viscosity for PP/PE10 with temperature range from 120 to 150℃ and shear rates from 1 to 100 hz.

Although rheometry was not able to be conducted for samples that contained aluminum powder due to the COVID-19 pandemic, the same relationships that were observed by Dermanci and Karabeyoglu [11] are expected to continue. The presence of aluminum powder does not inherently increase the viscosity of fuels, but the increased ratio of the polyethylene to paraffin does increase the viscosity.

5.2 Thermochemical Properties

5.2.1 Thermogravimetric Analysis

Thermogravimetric analysis (TGA) was conducted on all six compositions from room temperature to 800°C. Tests were conducted in both O_2 and N_2 environments to measure both the combustion and pyrolysis properties, respectively. Figure 21 shows the TGA thermal curves for all six compositions in the O_2 environment.

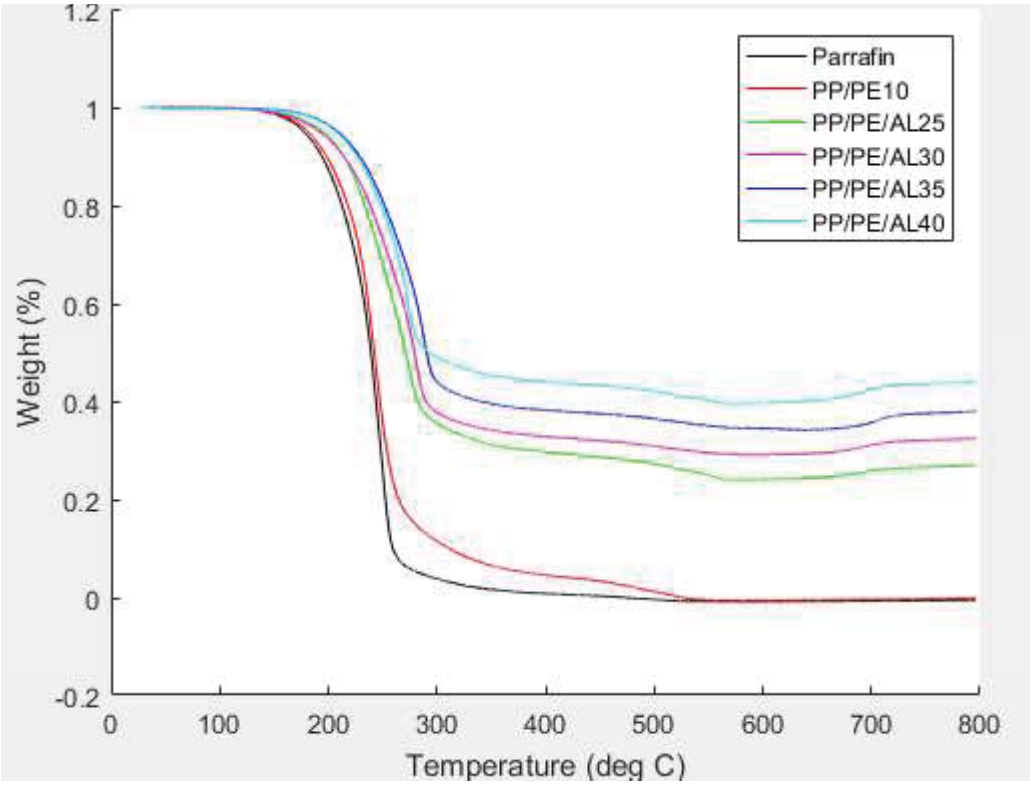

Figure 21: TGA in an O_2 environment.

One of the key differences between the data obtained between these tests and those collected by Hindustan University is that there was no observed decrease in the ignition temperature. As can be seen from Figure 21, each of the compositions begin to lose mass at relatively the same

temperature[3]. Each of the samples eventually decomposes to the mass percentage that corresponds to the percent of aluminum powder in the sample. The slight bump in the end corresponds to the oxidation of the aluminum powder and subsequent mass gain. The derivatives of each of the thermal curves (DTG) were also collected in Figure 22 in order to determine the maximum combustion rate.

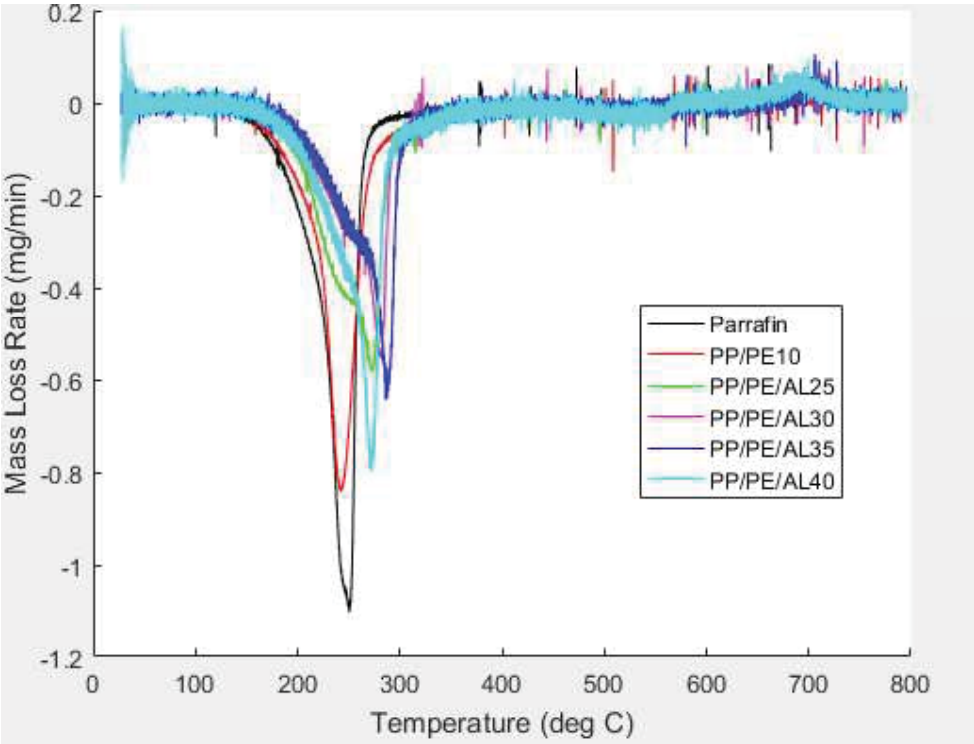

Figure 22: DTG of the compositions in an O_2 environment.

The sample that has the fastest combustion rate is pure paraffin followed by PP/PE10. A comparison of those samples containing aluminum powder shows that as the concentration of aluminum powder increases, the maximum combustion rate also increases as evidenced by the PP/PE/AL35 and PP/PE/AL40 samples. However, this trend is not perfectly consistent among all six of the fuel compositions.

TGA was also conducted in an N_2 environment to collect data on the pyrolysis of the fuel in Figure 23. This was used to obtain the initial decomposition temperature. The initial decomposition of the fuels begins at a higher temperature as the concentration of aluminum powder increases. This trend does not follow for the PP/PE/AL40 sample however. One potential explanation from this is that the aluminum powder veins contact other veins and transfer heat into the underlying fuel much more effectively than the other samples. Furthermore, these thermal curves were analyzed and further compounded into Table 5.

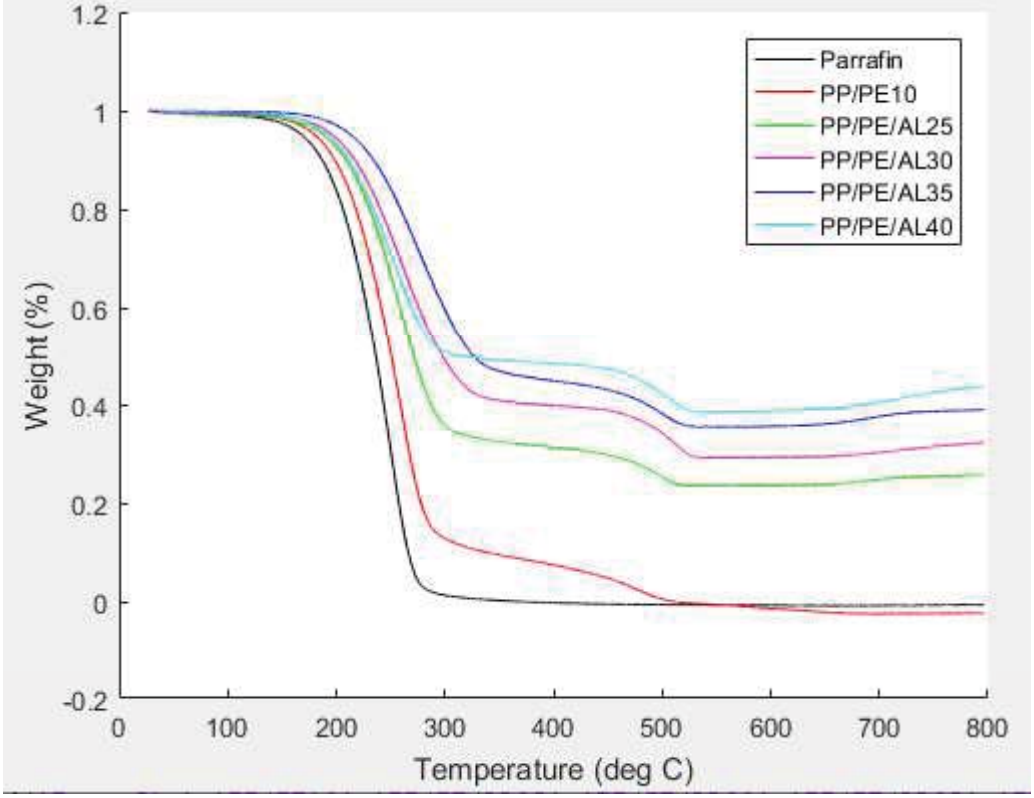

Figure 23: TGA in an N_2 environment.

Table 5: Collection of the thermochemical properties of each of the fuels from TGA.

Sample	T_d (℃)	T_{ig}(℃)	T_p(℃)	T_b(℃)	$\frac{dm}{dt}_{max}$ (mg/min)	t_{ig} (min)	t_{max} (min)	t_b (min)	X_i (x10^{-3})	X_c (x10^{-9})
PP	105	127	251	280	1.09	9.2	21.6	24.5	5.49	14.7
PP/PE	125	133	245	290	0.82	9.3	20.5	25.0	4.36	9.16
PP/PE/AL25	124	132	274	304	0.57	9.2	23.4	26.4	2.64	5.70
PP/PE/AL30	143	123	281	303	0.55	8.3	24.1	26.3	2.75	4.69
PP/PE/AL35	173	148	286	309	0.64	12.0	25.8	28.1	2.07	3.77
PP/PE/Al40	150	137	273	300	0.78	10.8	24.4	27.1	2.96	6.50

The trends in this data are not as clearly defined as in the data obtained by Hindustan University. The initial decomposition temperature and ignition temperature increases with the addition of more aluminum powder although this trend is not perfectly consistent throughout the compositions. The ignition and combustion parameters increase as the concentration of aluminum powder increases except in the case of the PP/PE/AL35 sample. The scanning electron microscope images of this sample shows that the veins of aluminum powder are not dispersed as

evenly as the other samples and the aluminum powder veins do not touch each other as much as the other samples. This means that the heat of the environment in the thermal analyzer does not transfer as well to the interior of the fuel sample as the other samples. From the compilation of this data, the pure paraffin still exhibits the most favorable ignition and combustion properties, but the PP/PE/AL40 sample has the most favorable properties of all of the samples that contain aluminum powder.

5.2.2 Differential Scanning Calorimetry

DSC was performed for each of the six compositions. Figure 24 depicts the thermal curves for the heat capacity as a function of temperature. The analysis was conducted in a nitrogen environment.

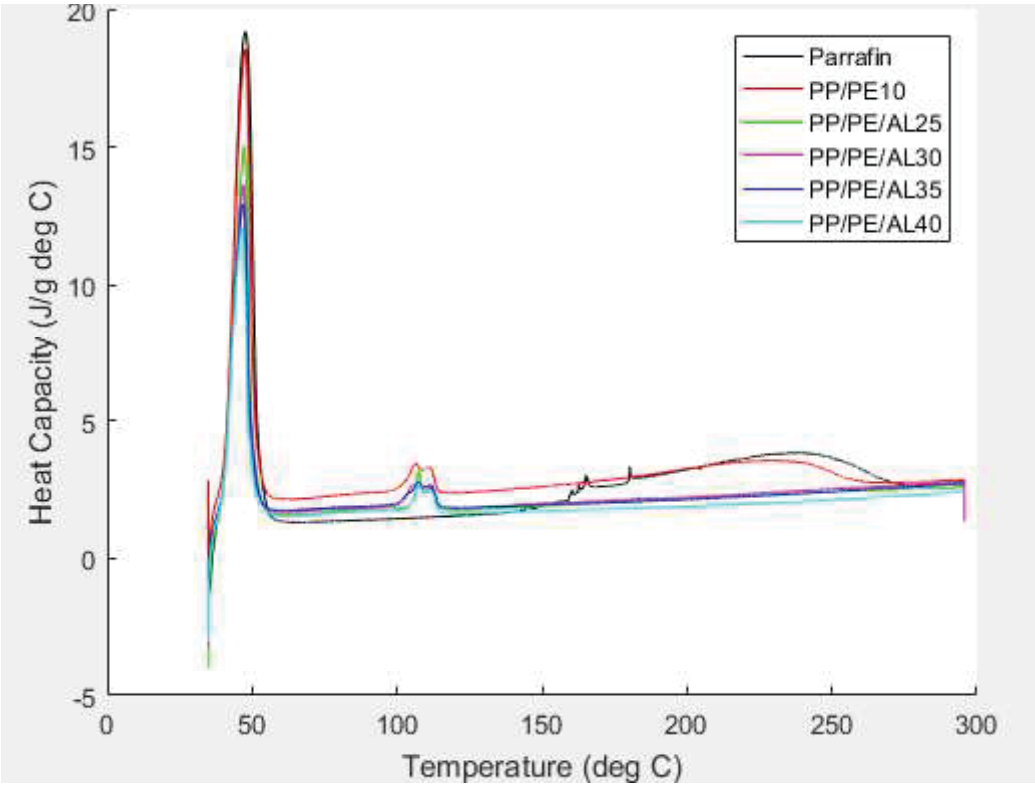

Figure 24: DSC curves for all six compositions in an N2 environment.

From the data it can be seen that the paraffin has a melting point of 47.6°C. The paraffin had a very narrow peak which means that the paraffin consisted of molecules of a similar length. This was not the case with the polyethylene as the melting point ranged from 106.1 to 111.3°C. Another trend shown is the increase in the heat capacity due to the addition of the polyethylene. With the additional increase in aluminum powder concentration, the heat capacity is increasingly lowered further to a point much closer to pure paraffin. A lower heat capacity is more desirable

as it will allow more of the heat generated from the combustion to be transferred to the underlying fuel grain resulting in a thicker liquid melt layer which allows the entrainment of more fuel droplets.

5.3 Hybrid Rocket Test Fire Results (Hypothesized)

[Due to the COVID-19 pandemic, the rocket motors were not able to be manufactured or tested.] It is quite difficult to predict the results that would have come from the test fires due to the complexity and dynamic nature of the physical processes that are involved in the internal combustion of the rocket, but from previous data, there are two potential and likely outcomes. The first potential outcome is that the aluminum greatly increases the energy released from the combustion of the fuel, which overcompensates for the increase in viscosity from the higher ratio of polyethylene to paraffin. The other potential outcome is that the large increase in viscosity would be the dominant factor and limit the regression rate. It is difficult to say which would be likely outcome for certain, but the results from the test fires conducted by Hindustan University shows that the regression rate increases with the increase in concentration of aluminum powder at a constant rate, which suggests that a further increase in aluminum powder concentration would lead to a higher regression rate.

6. Conclusion

Hybrid rocketry offers a unique solution to the dangers of solid and liquid rockets. By separating the oxidizer from the fuel, the risk of an explosion can be greatly reduced. This will allow for more safe space travel in the future. However, hybrid rockets have significant hurdles with a low regression rate since the fuel must first melt or vaporize and then become entrained in the oxidizer flow. With the introduction of liquefying paraffin-based fuels, small droplets of fuel can become entrained in the oxidizer flow due to the low viscosity of the melted fuel which leads to a much higher regression rate. However, these fuels lack the structural rigidity necessary to undergo a rocket launch; therefore, additives such as polyethylene and aluminum powder must be included in the fuel to increase the strength of these fuels. Aluminum powder also increases the regression rate of these fuels by increasing the energy released by the fuel when it burns and increasing the amount of heat that is transferred to the underlying fuel grain. This has been proven by previous experimentation conducted by Hindustan University, but has the potential to be further improved by the increase of additional aluminum powder in the fuel.

Three compressive yield tests were conducted for the six fuel samples. The PP/PE/AL40 sample had the highest compressive yield point and highest compressive Young’s Modulus. However, the PP/PE/AL40 samples started to exhibit a brittle failure mode which is more likely to lead to a catastrophic failure if there are stress concentrations inherent in the rocket motor from the casting process. Therefore, the sample with the best structural characteristics is the PP/PE/AL35 sample.

While the test fires and full rheometry test regimen were not able to be completed due to the COVID-19 pandemic, other thermochemical testing to include TGA and DSC were fully completed. From this data, it is a noticeable trend that the combustion and ignition properties of the fuel compositions increase with the further addition of aluminum powder, but they never quite reach the full potential of pure paraffin. Furthermore, the heat capacity of the fuel decreases with the addition of aluminum powder.

This analysis does not offer conclusive evidence as to which fuel sample would have the highest regression rate or characteristic velocity without conducting test fires, but due to the structural properties that were determined through compressive yield testing, it is a fair assessment that the PP/PE/AL35 sample is the most ideal sample to maximize the speed of combustion and ease of ignition of the fuel without entering into a brittle failure mode. This conclusion should be further validated by conducting test fires of the fuels with varying oxidizer flow rates.

7. Acknowledgements

Special thanks to Associate Professor Jin Kang and Instructor of Practical Applications Spencer Temkin for their wisdom and support with the project over the past year and a half. The project would have not achieved nearly what it has without their insight.

Additional thanks goes to Commander David Durkin, USN, for offering his knowledge on TGA/DSC and conducting the rheometry experiments, Captain Brad Baker, USN, for providing training on the Scanning Electron Microscope, Michael Spencer for conducting the compressive yield testing, and Dr. Eric Boyer and Dr. Grant Risha of Penn State University for their collaboration.

I would additionally like to thank Kelly Ruth for aiding in literature search, the USNA Machine Shop for providing their expertise at various points in the project and manufacturing the split molds, and MSC Graphics for their help in making the poster and assembling the report for this project.

8. References

[1] University of Waikato, "Science Learning Hub," 30 November 2011. [Online]. Available: https://www.sciencelearn.org.nz/images/412-hybrid-rocket-engine. [Accessed 27 December 2018].

[2] Stanford University, "Chapter 11: Hybrid Rockets," [Online]. Available:

https://web.stanford.edu/~cantwell/AA283_Course_Material/AA283_Course_Notes/AA283_Aircraft_and_Rocket_Propulsion_Ch_11_BJ_Cantwell.pdf. [Accessed 27 December 2018].

[3] Y. Pal and V. R. Kumar, "Physical and Ballistic Characterization of Aluminum-Loaded Paraffin Hybrid Rocket Fuels," *Energy & Fuels,* vol. 31, pp. 10133-10143, 2017.

[4] Marquardt, T., and Majdalani, J., "Review of Classical Diffusion-Limited Regression Rate Models in Hybrid Rockets," *Aerospace*, vol. 6, 2019, p. 75.

[5] M. J. 1. Chiaverini and K. K. Kuo, *Fundamentals of Hybrid Rocket Combustion and Propulsion.* Reston, Va: American Institute of Aeronautics and Astronautics, 2007*218.*

[6] S. Kim, J. Lee, H. Moon, H. Sung and J. Kim, "Empirical Estimation of Entrainment Regression Rate in Liquefying Solid Fuel for Hybrid Rocket Motor," in *47th AIAA/ASME/SAE/ASEE Joint Propulsion Conference & Exhibit*, San Diego, 2011.

[7] M. Kobald, C. Schmierer, H. K. Ciezki, S. Schlechtriem, E. Toson and L. T. D. Luca, "Viscosity and Regression Rate of Liquefying Hybrid Rocket Fuels," *Journal of Propulsion and Power,* vol. 33, no. 5, pp. 1245-1251, 2017.

[8] DONGYUA, "50ml Metal Veterinary Use Syringe Tuba Needle Tube Syringe Metal Syringe for Livestock Metal Shell Glass Needle Tube 21.5cm," [Online]. Available: https://www.amazon.com/DONGYUA-Veterinary-Syringe-Needle-Livestock/dp/B07Q37N8RX [Accessed 10 April 2020].

[9] Grainger, "HSTAT Series Silicone Heating Tape," [Online]. Available: https://www.grainger.com/product/13P848?gclid=Cj0KCQjw4dr0BRCxARIsAKUNjWSuZkU_IaFs0LrZUg99bMSTPwdeMAbOUp5we17OPSSnwNoi7QeQ2DkaAkHdEALw_wcB&cm_mmc=PPC:+Google+PLA&ef_id=Cj0KCQjw4dr0BRCxARIsAKUNjWSuZkU_IaFs0LrZUg99bMSTPwdeMAbOUp5we17OPSSnwNoi7QeQ2DkaAkHdEALw_wcB:G:s&s_kwcid=AL!2966!3!264974130409!!!g!388878740142! [Accessed 10 April 2020].

[10] Rocketarium, "1.1" Phenolic Tube," [Online]. Available: https://www.rocketarium.com/Build/Airframes/Phenolic/11?cPath=19_185& [Accessed 10 April 2020].

[11] O. Dermanci, A. M. Karabeyoglu, "Effect of Nano Particle Addition on the Regression

Rate of Liquefying Fuels," in *51th AIAA/ASME/SAE/ASEE Joint Propulsion Conference*; American Institute of Aeronautics and Astronautics, 2015.

9. Additional Sources

Sutton *et al*, *Rocket Propulsion Elements.* (9;9th; ed.) 2016;2017;.

G. Permutt, "Absolute Viscosity of The n-Paraffin Liquids," Newark College of Engineering, Newark, 1960.

Y. Pal, J. Baskar and S. Murugesan, "Testing of Paraffin-based Hybrid Rocket Fuel using Gaseous Oxygen Oxidiser," Defence Science Journal, vol. 62, no. 5, pp. 277-283, 2012.

PerkinElmer, "A Beginner's Guide to Thermogravimetric Analysis," 2015. [Online]. Available: https://www.perkinelmer.com/lab-solutions/resources/docs/faq_beginners-guide-to-thermogravimetric-analysis_009380c_01.pdf. [Accessed December 30 2018].

PerkinElmer, "Differential Scanning Calorimetry (DSC)," 2014. [Online]. Available: https://www.perkinelmer.com/CMSResources/Images/44-74542GDE_DSCBeginnersGuide.pdf. [Accessed 2 January 2019].

M. Z. Akhter and M. A. Hassan, "Characterisation of paraffin-based hybrid rocket fuels loaded with nano-additives," *Journal of Experimental Nanoscience: Nanomaterial Reinforced Hybrid Composites and their Applications (ICMPC 2018),* vol. 13, *(sup1),* pp. S31-S44, 2018.

I. Nakagawa and S. Hikone, "Study on the Regression Rate of Paraffin-Based Hybrid Rocket Fuels," *Journal of Propulsion and Power,* vol. 27, *(6),* pp. 1276-1279, 2011.

American Institute of Aeronautics and Astronautics, "Small-scale gaseous oxygen hybrid rocket testing for regression rate and combustion efficiency studies," in Anonymous American Institute of Aeronautics and Astronautics, 2017, pp. 1-1.

S. Kim *et al*, "Evaluation of Paraffin–Polyethylene Blends as Novel Solid Fuel for Hybrid Rockets," *Journal of Propulsion and Power,* vol. 31, *(6),* pp. 1750-1760, 2015.

A. Karabeyoglu *et al*, "Scale-Up Tests of High Regression Rate Paraffin-Based Hybrid Rocket Fuels," *Journal of Propulsion and Power,* vol. 20, *(6),* pp. 1037-1045, 2004.